24th COBEM - 2017

24th ABCM International Congress of Mechanical Engineering
December 3-8, 2017, Curitiba, PR, Brazil

COBEM-2017-1073
EXPERIMENTAL VALIDATION BY ULTRASONIC TECHNIQUE OF THE NUMERICAL ANALYSIS OF AN ASCENDANT FLOW UNDER THE INFLUENCE OF THE CENTRIFUGAL AND GRAVITATIONAL FIELDS

Henrique K. Eidt
Carolina C. Rodrigues
Rafael Dunaiski
César Y. Ofuchi
Paulo H. D. Santos
Flávio Neves
Rigoberto E. M. Morales
Multiphase Flow Center (NUEM), Federal University of Technology - Paraná (UTFPR) – Rua Deputado Heitor Alencar Furtado 5000, Bloco N, CEP 81280-340, Curitiba, Brazil
hkeidt@gmail.com, carolcimarelli@gmail.com, rafael.dunaiski@gmail.com, cesarofuchi@gmail.com, psantos@utfpr.edu.br, neves@utfpr.edu.br, rmorales@utfpr.edu.br

Abstract. *In the process of oil extraction and production, several patterns of liquid-gas two-phase flow can occur. The efficiency of this process can be greatly increased with the use of equipment capable of performing phase separation, if possible still on the seabed. Such devices, known as separators, usually have high separation efficiency but its generally elevated size can be prejudicial. Therefore, a device capable of dividing the flow into more separators has been developed, enabling smaller separation equipment to be used while and thus facilitating installation, maintenance, and construction. The distribution system here studied has a cyclonic chamber, in which an upward liquid film flow is formed under the influence of the centrifugal and gravitational fields. The development of the liquid film flow is numerically analyzed using ANSYS-CFX and an experimental bench was built in order to validate the numerical model. The experimental data were obtained using an ultrasound technique and a comparison with the numerical model yielded a maximum difference of 38.9% in the value of the average liquid film thickness inside the cyclonic chamber.*

Keywords: *distribution system, cyclonic chamber, ascendant liquid film flow, ultrasound technique, numerical model.*

1. INTRODUCTION

The extraction and production of oil in deep water has increased recently, becoming almost 1/3 of all world production (Morais, 2013). Usually, multiphase flow is present in this process, which can be simplified as a two-phase liquid-gas flow. In order to increase production, the phases can be separated still at the bottom of the seabed. To perform this process, equipment called separators are employed. An example of such equipment is VASPS (Vertical Annular Separation and Pumping System). This device has a high efficiency regarding the separation rate and is up to five times faster than conventional gravitational separators (Stel et *al.*, 2012). However, the VASPS has large dimensions (approximately 30 m high) which can hamper installation procedures, maintenance and construction. Figure 1 shows the schematic representation of the VASPS liquid-gas separator positioned in the seabed. The sea oscillations coupled with the high length of the equipment can cause damage to the structure or influence the separation rate (Storti, 2013).
In this sense, studies were performed to develop a distribution system capable of dividing the liquid and gas flows into more separators, with smaller dimensions, without affecting the separation efficiency. The distribution system consists of two inlets, a cyclone chamber and the distribution channels (outlets), as can be seen in Figure 2. The tangential positioning of the inlets combined with the curvature of the cyclonic chamber leads to the formation of a centrifugal field. Due to this field and to differences in gas and liquid density, the liquid phase is displaced near the chamber wall while the gas flows in the region of the axial core. Such flow is characterized by an ascendant liquid film flow under the influence of the centrifugal and gravitational fields.

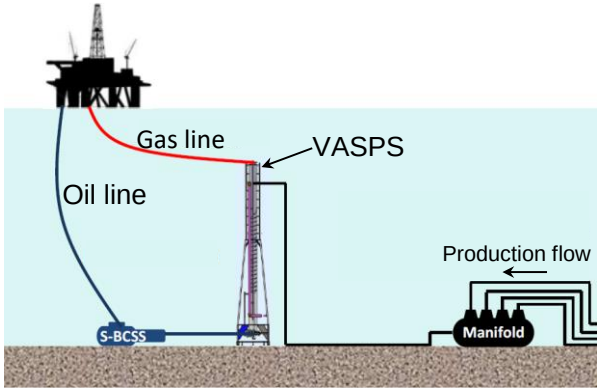

Figure 1. Schematic representation, off-scale, of the liquid-gas two-phase separator VASPS in the seabed.

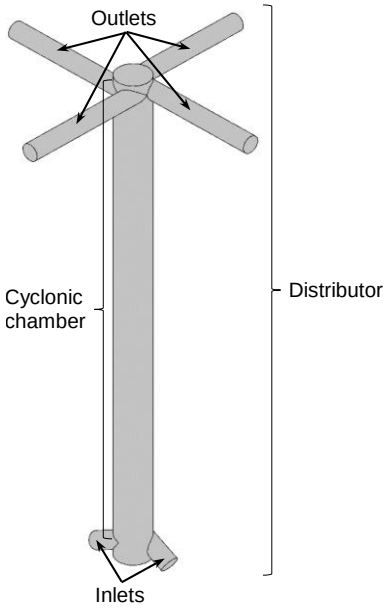

Figure 2. Distribution system with four outlets, a cyclonic chamber and two inlets.

The main goal of this study is to model numerically the complex phenomenon regarding to ascendant two-phase flow under the influence of the centrifugal and gravitational fields. In order to increase the reliability of theoretical results, the model was validated in comparison with experimental results, which were obtained by ultrasonic technique. The numerical model solves the conservation equations for mass and momentum in order to determinate the flow's development and behavior inside the cyclonic chamber.

2. EXPERIMENTAL AND NUMERICAL PROCEDURE

2.1 Experimental Setup

The experimental loop consists of an acrylic pipe of 8 m length and 26 mm diameter as well as associated devices to produce two-phase water-air flow under controlled conditions (Figure 3(a)). Tap water is circulated in a closed loop through a pump. Air flow is produced by a compressor and stored in a vessel. Air and water flow rates are independently measured by flow meters. The air coming from the vessel compressor is mixed with the flowing water in the pipe entrance through a gas-liquid mixer. The pipe ends in a vertical direction, at a cyclonic chamber entrance where the flow is divided and mixed again. The mixture is separated at a water tank which expels air to the atmosphere and stores the water. In order to obtain the exact air flow rate at the measurement point, a rotameter is used, and its readings are compensated by the pressure difference at the pipe entrance and the pressure at the measurement point. Temperatures and pressures are monitored using industrial sensors connected by Foundation Field Bus network. The water flow rate is controlled by a frequency inverter and a LabVIEW program from a National Instrument acquisition system. Liquid film thickness is measured using the ultrasonic setup described in Figure 3(b). A pulser/receiver model Olympus 5077PR and a Keysight Oscilloscope model MSOS104A are used to generate and digitize ultrasonic data.

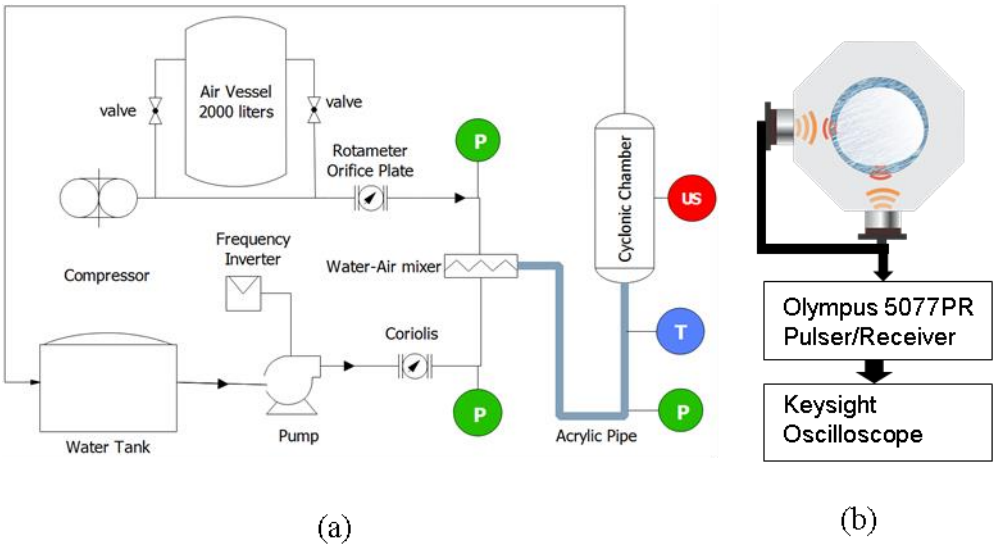

Figure 3: (a) Schematic representation of the measurement plant with the ultrasound sensors (US), pressure and temperature sensors (P) and (T). (b) Ultrasonic setup installed at the experimental rig.

In order to determine the thickness of the liquid film from the ultrasound acquisition system, the pulse-echo principle was used to measure the transit time of an acoustic pulse from its emission (pulse) to its return (echo). Figure 4 (a) illustrates the process. The ultrasound equipment uses a piezoelectric effect sensor as the emitter and receiver.

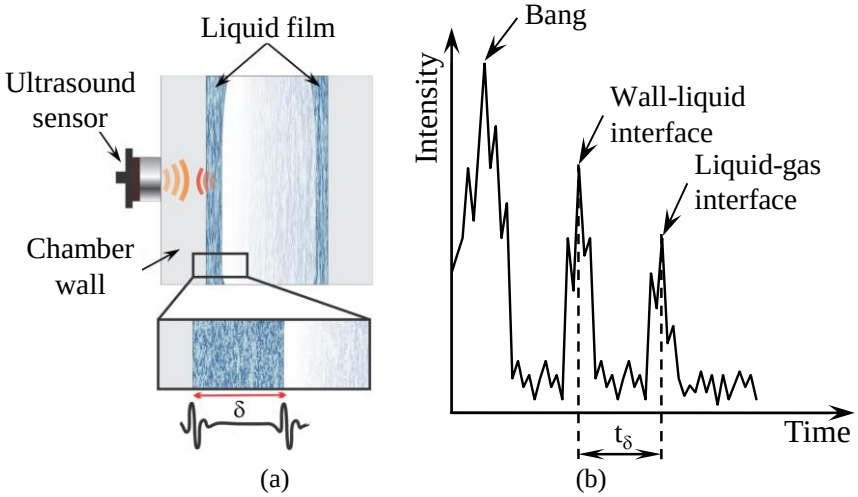

Figure 4. (a) Pulse-echo principle representation at cyclonic chamber. (b) Ultrasound receiver signal.

In the process of determining the liquid film thickness, the mechanical wave is first reflected at the wall-liquid interface and secondly at the liquid-gas interface, as illustrated in Figure 4(b), which presents the received signal intensity as a function of time during the measurements for each channel. Three peaks are observed: the first refers to the sensor initial shoot; the second relates to the wave reflected at the wall-liquid interface and the last one relates to the liquid-gas interface. This last peak varies with time due to flow's interfacial waves structure (Case, 1998).

The film thickness, δ, is calculated using the sound speed in liquid, c, and the time it took the wave to go through the film twice, t_δ:

$$\delta = c\left(\frac{t_\delta}{2}\right) \tag{1}$$

After acquisition, the data was analyzed using MATLAB software. The ultrasonic measurements were made in a single day in two perpendicular points at a height of 190 mm from the bottom of the cyclonic chamber. Therefore, time averaged film thickness values were analyzed for each case at the same plane.

2.2 Numerical Model

Numerical simulations were performed for a mixture of water and air. The inlet condition was set within a range of superficial velocities of air (JG) and water (JL), which are defined as:

$$JG = \frac{Q_G}{A_P} \tag{2}$$

$$JL = \frac{Q_L}{A_P} \tag{3}$$

where A_P is the cross section area of the pipe and Q is the volumetric flow rate of each phase. Values of both, JG and JL were varied from 0.5 to 2.0 m/s.
The numerical model was developed and implemented using the ANSYS–CFX software package. Flow is turbulent and the shear stress transfer model (SST) was applied. The flow was considered transient, isothermal and incompressible. Due to the two-phase characteristic of the flow, an inhomogeneous Eulerian-Eulerian model was applied. This model is described by ANSYS, 2015 and it is a mass weighted approach. Phases are considered as continua and interpenetrating. If non-drag forces and interfacial mass transfer between the phases are neglected, the governing equations for this case can be written as:

$$\frac{\partial}{\partial t}\left(r_i \rho_i\right) + \nabla \bullet \left(r_i \rho_i \vec{V}_i\right) = 0 \tag{4}$$

$$\frac{\partial}{\partial t}\left(r_i \rho_i \vec{V}_i\right) + \nabla \bullet \left(r_i \rho_i \vec{V}_i \times \vec{V}_i\right) = \nabla\left(r_i \mu_i \left(\nabla \vec{V}_i \times \left(\nabla \vec{V}_i\right)_T\right)\right) - r_i \nabla p + r_i \rho_i \vec{g} + \vec{F}_D \tag{5}$$

where V_i is the velocity of the phase i, r_i is the volume fraction of the phase, ρ_i is the density, μ_i the viscosity, ∇p the pressure gradient, g the gravity acceleration and FD the drag force between the phases.
During the numeric model development, some simplifications regarding the flow were required. Therefore, were adopted:

i. Water was used for liquid phase and air for gas phase for both numerical simulation and experimental bench;
ii. The initial condition considered was the geometry with only liquid phase velocity equal zero;
iii. Isothermal (300K) and no-slip wall boundary conditions;
iv. Turbulent intensity equals to 5%, which is equivalent to a viscosity ratio equals to $\nu_t/\nu = 10$;
v. Opening condition at outlets, $\Delta P_{openning} = 0$;
vi. Slug flow were set at the inlets, and one representative unit cell for each case. The values for frequency, length and quantity for each phase at the long bubble and the liquid slug were obtained experimentally.
vii. The following equation was used to calculate the time averaged liquid film thickness at a transversal plane at 190mm from the bottom of the cyclonic chamber:

$$\bar{\delta} = R_0\left(1 - \sqrt{\alpha}\right) \tag{6}$$

where R_0 is the cyclonic chamber radius and α is the time averaged gas volumetric fraction at the transversal plane.
viii. Hybrid mesh were used for the model, with tetrahedral volume mesh at the inlets region, and hexahedral volume mesh at the cyclonic chamber, with mesh refinement near the walls as required by the turbulence model SST, as shown at the Figure 5. The number of elements (2,126,817) required so the liquid film thickness is not influenced by the number of elements were determined through mesh test. Since it is an oscillatory flow, the total simulation time is 1 s. At least, the time step adopted is 0.002 s.

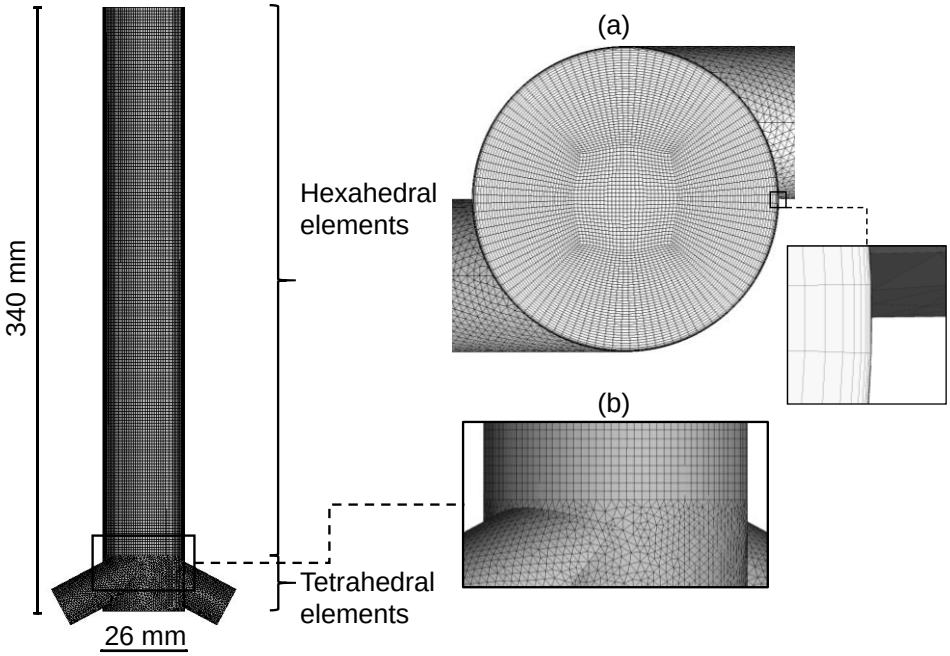

Figure 5: Numerical mesh used: (a) Near-wall mesh refinement representation. (b) Merging two kinds of mesh elements.

3. RESULTS AND DISCUSSION

In order to validate the numerical model, the time averaged liquid film thickness at a transversal plane at 190 mm from the bottom of the cyclonic chamber was compared with experimental results. Ten representative cases were chosen varying the superficial gas velocity and the superficial liquid velocity. When these velocities are combined for an ascendant flow inside a 25,4 mm diameter horizontal pipe, slug flow are obtained, accordingly to flow-pattern map found in Barnea (1986). Slug flow was chosen due to its large occurrence in oil extraction process and it least chance to be equally divided at the outlets. However, when a centrifugal field is imposed to the flow, the distribution equitability is improved.

The thickness of the liquid film inside the cyclonic chamber in the experimental bench was obtained by the ultrasonic technique and the results were compared with numerical results, which is shown in Tab. 1. Accordingly, it is possible to state that most analyzed cases are good approximations to the experimental results, with seven cases within a range of 25%. It may be noted that the biggest difference between the experimental and numerical results is 38.5%. This is due to the fact that liquid film thicknesses have relatively low values and any small variation corresponds to a significant percentage variation.

Table 1 – Comparing the numerical results with the experimental data.

Cases	*JL [m/s]*	*JG [m/s]*	*Numerical* δ *[mm]*	*Experimental* δ *[mm]*	*Difference*
1	0.5	0.5	8.63	6.62	23.2%
2	1.0	0.5	9.29	8.21	11.7%
3	1.0	1.0	8.10	5.94	26.7%
4	1.0	1.5	6.94	4.41	36.4%
5	1.0	2.0	5.83	3.57	38.5%
6	1.5	0.5	8.97	8.53	1.0%
7	1.5	1.0	7.19	5.91	17.8%
8	1.5	1.5	3.97	4.20	5.6%
9	2.0	0.5	7.95	8.06	1.5%
10	2.0	1.0	4.13	4.56	10.6%

Figure 6 shows the points of the differences between the experimental and numerical data of the liquid film thickness. In order to improve visualization, the points were normalized. It is noted that most of the values obtained are between $\pm$25%. Since simplifications were adopted in order to validate the numeric model, the results may be considered precise. Furthermore, the experimental results contain some errors due to lack of precision of the measuring equipment. Therefore,

numerical results are reliable for this operation range, supporting the understanding of the flow inside the cyclonic chamber.

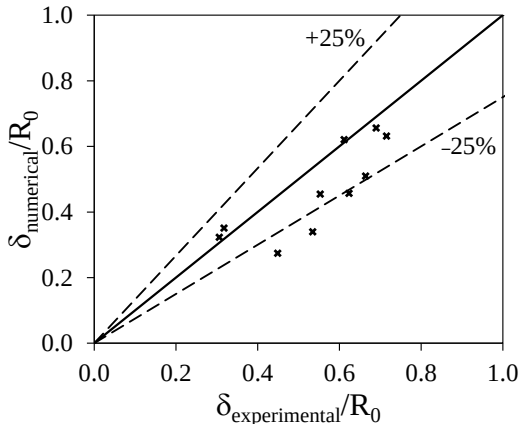

Figure 6: The behavior of differences in numerical and experimental results plotted with a 25% error.

By performing a numerical analysis in a group of specific cases, with JL = 1.0 m/s and varying JG from 0.5 up to 2.0 m/s, the following behaviors can be observed. Figure 7-(a) shows the behavior of the gas volume fraction along the cyclonic chamber as well as time average streamlines in the analyzed cases. The liquid phase is represented by color blue and the gas phase by color red. The gas volume fraction, in Figure 7-(a), increases (or the liquid film thickness reduces) as the gas velocity increase. This occurs because the increment in velocity increases the mass flow rate of the gas, so the volume of the gas phase occupies more space in the cyclonic chamber, thereby reducing the thickness of the liquid film. At the entrance of the cyclonic chamber, the flow is influenced by the tangential inlets, so the centrifugal force is more intense. As the flow passes through the chamber, the tangential and axial velocities decrease, but the tangential velocity decreases faster than the axial velocity. Because of this, the angle of the streamlines to the horizontal increases as the flow flows through the chamber, this phenomenon is more easily visualized in the case of JG = 0.5 m / s.

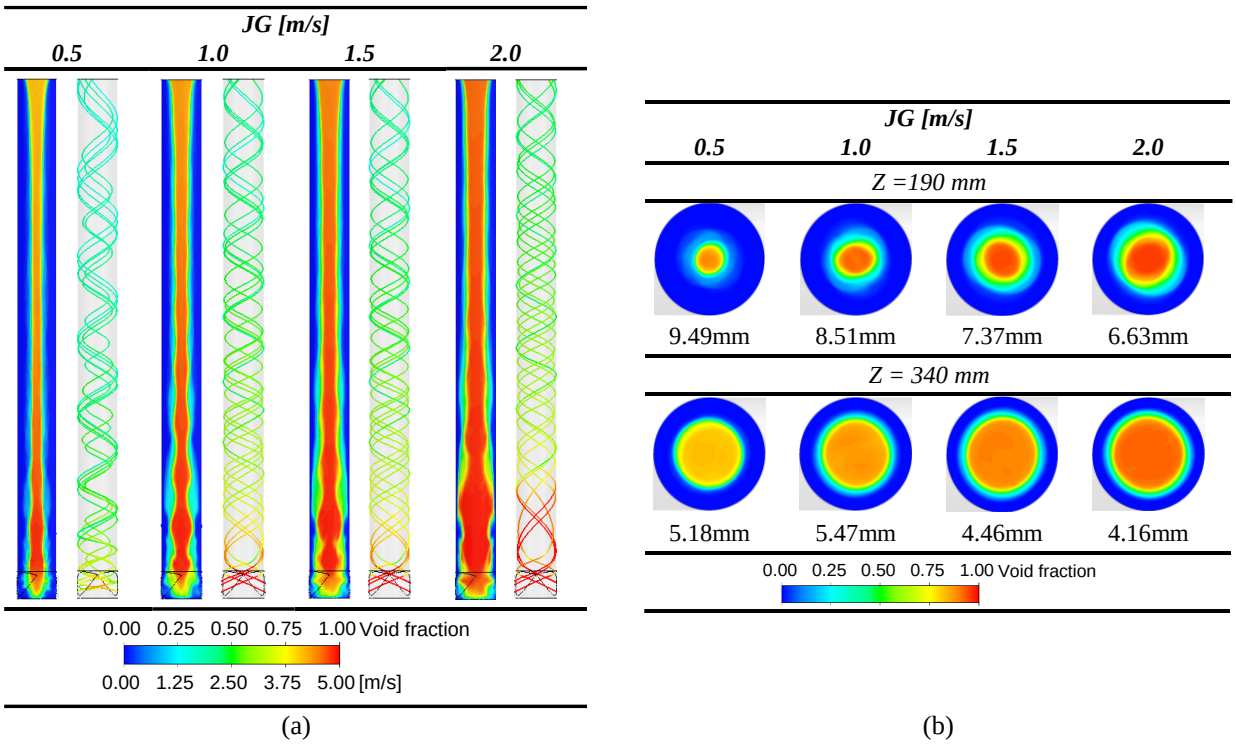

Figure 7: (a) Time average behavior of the liquid film into cyclone chamber for the liquid velocity equal 1.0 m/s; (b) Time average behavior of the liquid film in cross sections for fixed liquid velocity equal 1.0 m/s.

Figure 7-(b) shows the time average behavior of the liquid film in cross sections, 190 mm and 340 mm, for fixed liquid velocity equal 1.0 m/s. It can be seen that as the gas velocity increases, the thickness of the liquid film in the cross sections decreases. It is also observed that at Z = 190 mm the liquid film is not uniformly distributed across the cross section,

however, at a height of 340 mm, the liquid film has a uniform thickness throughout the section. This implies that the height of the cyclonic chamber is essential for the flow of the liquid film to develop and become axisymmetric.

4. CONCLUSIONS

From the presented results it can be affirmed that the numerical model developed in this study can effectively represent the flow inside the cyclonic chamber of the distribution system. Thus, the numerical model can provide more detailed information on variables that control the ascendant flow of liquid film that occurs in the cyclonic chamber, allowing the development of more efficient distribution and separation systems.

5. AKNOWLEDGMENTS

The authors acknowledge the UTFPR, NUEM and PETROBRAS for the infrastructure, support and assistance for the development of this study.

6. REFERENCES

Morais, J. M. de, Offshore petroleum (in Portuguese), Institute of Applied Economic Research (IPEA), Rio de Janeiro, Brazil (2013). 424p. ISBN: 978-85-7811-159-5.

Stel H, Ofuchi EM, Franco AT, Genaro JG, Morales REM. Numerical study of the free surface flow in a centrifugal gas-liquid separator. ASME International Mechanical Engineering Congress and Exposition, Texas, USA. 2012.

Storti, F.C., Experimental Study of Separation Efficiency of the VASPS Separator Expansion Chamber, Doctoral Thesis in Engineering. Campinas State University, Brazil. 2013.

Case, Terrence D.: Ultrasound Physics and Instrumentation. Surgical Clinics of North America. Department of Surgery, University of Vermont, Burlington, Vermont, 1998.

Ansys, "ANSYS - Solver Theory Guide", ANSYS Inc., Canonsburg, PA, USA. 2015.

7. RESPONSIBILITY NOTICE

The authors are the only responsible for the printed material included in this paper.